

## Blocking SLC7A11 attenuates the proliferation of esophageal squamous cell carcinoma cells

Wen-Ting Li<sup>a\*</sup>, Xin Jin<sup>a\*</sup>, Sheng-Jie Song<sup>a</sup>, Chong Wang<sup>a</sup>, Chuang Fu<sup>a</sup>, Wen Jiang<sup>b</sup>, Jie Bai<sup>a</sup> and Zhi-Zhou Shi<sup>a</sup>

<sup>a</sup>Medical School, Kunming University of Science and Technology, Kunming, People's Republic of China; <sup>b</sup>Department of Thoracic Surgery, The First People's Hospital of Yunnan Province & The Affiliated Hospital of Kunming University of Science and Technology, Kunming, People's Republic of China

### ABSTRACT

The role of ferroptosis-associated gene SLC7A11 in esophageal cancer progression is largely unknown, therefore, the effects of blocking SLC7A11 on esophageal squamous cell carcinoma (ESCC) cells are evaluated. Results showed that SLC7A11 was overexpressed in ESCC tissues both in mRNA and protein levels. Blocking SLC7A11 using Erastin suppressed the proliferation and colony formation of ESCC cells, decreased cellular ATP levels, and improved ROS production. Sixty-three SLC7A11-binding proteins were identified using the IP-MS method, and these proteins were enriched in four signaling pathways, including spliceosome, ribosome, huntington disease, and diabetic cardiomyopathy. The deubiquitinase inhibitors PR-619, GRL0617, and P 22077 could reduce at least 40% protein expression level of SLC7A11 in ESCC cells, and PR-619 and GRL0617 exhibited suppressive effects on the cell viability and colony formation ability of KYSE30 cells, respectively. Erastin downregulated GPX4 and DHODH and also reduced the levels of  $\beta$ -catenin, p-STAT3, and IL-6 in ESCC cells. In conclusion, SLC7A11 was overexpressed in ESCC, and blocking SLC7A11 using Erastin mitigated malignant phenotypes of ESCC cells and downregulated key ferroptosis-associated molecules GPX4 and DHODH. The therapeutic potential of targeting SLC7A11 should be further evaluated in the future.

### ARTICLE HISTORY

Received 20 January 2024  
Revised 26 March 2024  
Accepted 18 April 2024

### KEYWORDS

SLC7A11; Erastin; ESCC; GPX4

## Introduction


Esophageal cancer (EC) is one of the most common malignant tumors and ranks eighth in the world (Han et al. 2023). EC consists of two histological types: esophageal squamous cell carcinoma (ESCC) and esophageal adenocarcinoma (EAC) (Deng et al. 2023), and more than 90% of all EC patients are ESCC, the main subtype in China (Yang et al. 2020). Although the therapeutic methods for ESCC have been advanced, however, the prognosis is still entirely unfavorable with a 5-year survival rate of just 25% (Shu et al. 2022). Thus, exploring the underlying mechanisms of esophageal progression is quite urgent and important.

Ferroptosis first reported in 2012, is a novel mode of cell death different from apoptosis, necrosis, and autophagy and has the characteristics of intracellular iron accumulation and lipid peroxidation (Dixon et al. 2012). Solute carrier family 7 member 11 (SLC7A11) and solute carrier family 3 member 2 (SLC3A2) form

the system Xc<sup>-</sup> which exchanges cystine and glutamate across the cell membrane and leads to glutathione (GSH) synthesis (Sato et al. 2000). SLC7A11 is often abnormally overexpressed in many cancers (Koppula et al. 2018). SLC7A11 was overexpressed in ESCC tissues, and its high expression was correlated with lymph node metastasis in ESCC patients. Mechanically, nuclear factor erythroid-2 (NRF2) bound with the promoter of SLC7A11 and potentiated its transcription (Feng et al. 2021). Another study revealed that SLC7A11 was predominantly expressed in the nuclei of ESCC cells and its positive expression indicated poor prognosis independently. Functionally, silencing SLC7A11 arrested the G1/S transition of ESCC cells (Shiozaki et al. 2014). SLC7A11, which was targeted and negatively regulated by miR-513a-3p, was also involved in the resistance caused by lncRNA BBOX1-AS1 to ferroptosis (Pan et al. 2022). Ferulic acid could mitigate malignant phenotypes of ESCC cells via decreasing SLC7A11/glutathione

**CONTACT** Zhi-Zhou Shi  zhizhoushi@126.com  Medical School, Kunming University of Science and Technology, Kunming, 650500, People's Republic of China; Wen Jiang  89480226@qq.com  Department of Thoracic Surgery, The First People's Hospital of Yunnan Province & The Affiliated Hospital of Kunming University of Science and Technology, Kunming, 650000, People's Republic of China; Jie Bai  jiebai662001@126.com  Medical School, Kunming University of Science and Technology, Kunming, 650500, People's Republic of China

\*Contributed equally.

 Supplemental data for this article can be accessed online at <https://doi.org/10.1080/19768354.2024.2346981>.

© 2024 The Author(s). Published by Informa UK Limited, trading as Taylor & Francis Group

This is an Open Access article distributed under the terms of the Creative Commons Attribution-NonCommercial License (<http://creativecommons.org/licenses/by-nc/4.0/>), which permits unrestricted non-commercial use, distribution, and reproduction in any medium, provided the original work is properly cited. The terms on which this article has been published allow the posting of the Accepted Manuscript in a repository by the author(s) or with their consent.

peroxidase 4 (GPX4) and leading to ferroptosis (Cao et al. 2022). The expression of SLC3A2 was also reported to be linked with the survival time of ESCC patients (Zhao et al. 2022). Erastin is a widely used SLC7A11 inhibitor and ferroptosis inducer and markedly leads to ferroptosis of several types of cancer cells such as pancreatic cancer cells, oral squamous cell carcinoma cells, and so on (Wang et al. 2023; Zerbato et al. 2023). Nonetheless, its effects on ESCC cells are still absolutely unclear.

In this study, we first analyzed the expression levels of SLC7A11 in ESCC tissues, then evaluated the suppressive effects of an SLC7A11 inhibitor Erastin on ESCC cells, and eventually identified the SLC7A11 interactome and the deubiquitinases which regulated SLC7A11 expression and also assessed downstream critical molecules.

## Materials and methods

### Patients and tissue samples

Ten ESCC samples were obtained from the First People's Hospital of Yunnan Province and the Affiliated Hospital of Kunming University of Science and Technology. Informed consent was signed by every patient, and the Medical Ethics Committee of Kunming University of Science and Technology approved this study.

### Cell lines and cell cultures

Human ESCC cell lines (KYSE30, KYSE70, KYSE140, KYSE150, KYSE180, KYSE450, KYSE510, TE1, TE10, EC109) and human esophageal normal cell line (Het-1A) were cultured in RPMI-1640 medium supplemented with 10% fetal bovine serum at 37°C and 5% CO<sub>2</sub>. The deubiquitinase inhibitor library and Erastin were obtained from MedChemExpress.

### Cell viability and colony formation assays

Cell viability and colony formation detections were carried out following our previous study (Shi et al. 2020).

### ATP detection

Cellular ATP level was detected using an enhanced ATP detection kit (Beyotime, S0027) according to the manufacturer's instructions. After Erastin treatment (0, 50, 100 μM) for 24 hours, KYSE30 and KYSE510 cells were collected and ATP levels were measured.

### Reactive oxygen species detection

Reactive oxygen species (ROS) concentrations were analyzed using the Reactive Oxygen Species Assay Kit

(Beyotime, S0033S) according to the manufacturer's instructions. Fluorescence microscopy was used to assess the ROS levels.

### Western blotting assay

Western blotting assay was performed following our previous study (Shi et al. 2020). The antibody information is as follows: anti-SLC7A11 (ab175186, abcam), anti-GAPDH (ab8245, abcam), anti-GPX4 (ab125066, abcam), anti-p-STAT3 (9134, cell signaling technology), anti-IL-6 (21865-1-AP, proteintech), anti-β-catenin (8480, cell signaling technology), anti-ELAVL1 (11910-1-AP, proteintech), anti-DHODH (14877-1-AP, proteintech), anti-DRP1 (12957-1-AP, proteintech), anti-MFN1 (13798-1-AP, proteintech) and anti-PKM2 (4053, cell signaling technology).

### Immunohistochemistry assay

Immunohistochemical staining was performed according to our previously reported method (Shi et al. 2020). SLC7A11 antibody (ab307601, abcam) was used in this assay.

### IP-MS assay

KYSE30 and KYSE510 cells were prepared using IP lysis buffer (Thermo, USA), and an immunoprecipitation procedure was carried out. SLC7A11 antibody (ab175186, abcam) and Fast Silver Stain Kit (Beyotime, China) were utilized to capture the SLC7A11-binding proteins and stain gels to visualize proteins, respectively. Then, peptides were extracted, concentrated, and detected using LC-MS/MS (Q Exactive mass spectrometer, Thermo).

Gene annotation (GO) and Kyoto Encyclopedia of Genes and Genomes (KEGG) pathway analyses were conducted using DAVID software (<https://david.ncifcrf.gov>) and the SangerBox online platform (<http://vip.sangerbox.com/home.html>) based on SLC7A11-binding proteins. Protein-Protein Interaction (PPI) network was constructed using the STRING website (<https://cn.string-db.org>), and hub genes were analyzed using cytoHubba plugins in Cytoscape.

### Datasets analysis

Datasets of ESCC (GSE53622 and GSE53624), colorectal cancer (CRC, GSE113513) and head and neck squamous cell carcinoma (HNSCC, GSE36110) from Gene Expression Omnibus (GEO) database (<https://www.ncbi.nlm.nih.gov/gds>) were harnessed to analyze the expression level of SLC7A11 in different cancers. GEPIA

(<http://gepia2.cancer-pku.cn/#index>) was applied to evaluate the expression level of SLC7A11 in cancers.

### Statistical analysis

Data is presented as the mean  $\pm$  SD and analyzed by GraphPad Prism software (version 9.0). One-way ANOVA and Student's *t*-test are applied to analyze the data.  $p < 0.05$  was defined as statistically significant.

## Results

### SLC7A11 was overexpressed in ESCC tissues

The mRNA expression levels of SLC7A11 in ESCC and CRC tissues were higher than those in adjacent normal tissues (Figure 1A-1C), and SLC7A11 was also overexpressed in KRAS mutated HNSCC tissues than in KRAS wild-type tissues (Figure 1D) based on the datasets (GSE53622, GSE53624, GSE113513, and GSE36110) from Gene Expression Omnibus (GEO) database. The TCGA data (from the GEPIA database) showed that SLC7A11 was highly expressed in COAD (Colon adenocarcinoma), ESCA (Esophageal carcinoma), LUSC (Lung squamous cell carcinoma), READ (Rectum adenocarcinoma) and UCEC (Uterine corpus endometrial carcinoma, Figure 1E). The positive staining of SLC7A11 was detected in 3 of 10 ESCC tissues, with negative staining in adjacent normal tissues by analyzing using the immunohistochemistry (IHC) method (Figure 1F). Western blotting results further indicated that 2 out of 4 cases had elevated protein levels of SLC7A11 (Fold change  $> 2.0$ ) in ESCC tissues than corresponding normal tissues (Figure 1G).

### Blocking SLC7A11 suppressed the proliferation of ESCC cells

Compared with human esophageal normal cells (Het-1A), SLC7A11 protein expression was augmented in KYSE30, KYSE150, KYSE180, KYSE450, KYSE510 and TE1 ESCC cells (Figure 2A). Erastin is a widely used inhibitor of SLC7A11 and is applied to assess the effects of SLC7A11 inactivation on tumorigenic phenotypes of ESCC cells. Erastin decreased cell viabilities of KYSE30, KYSE150, KYSE180, KYSE510, TE1, TE10, and Het-1A cells; the cell viabilities of KYSE30, KYSE180, KYSE510 and TE1 treated with 100  $\mu$ M Erastin were below 50%, however, 1  $\mu$ M to 100  $\mu$ M Erastin didn't affect the cell viability of KYSE450 cells showing resistance to Erastin (Figure 2B-2I). Erastin also remarkably suppressed the colony formation of KYSE30 and KYSE510 cells (Figure 2J and 2K). Interestingly, Erastin reduced the ATP levels

and enhanced ROS levels in KYSE30 and KYSE510 cells (Figure 2L-2Q).

### Identification of SLC7A11 interactome in ESCC cell lines

IP-MS technology is harnessed to identify the SLC7A11 interactome in KYSE30 and KYSE510 ESCC cells (Figure 3A). Using IgG as the negative control, 63 SLC7A11 specific binding proteins were identified both in KYSE30 and KYSE510 cells (Table 1). Next, GO and KEGG pathway enrichment analyses were conducted using DAVID software and the SangerBox online platform based on SLC7A11 interacted proteins (Figure 3B-3E, Table S1 and S2). The top five terms in biological processes (BP) analysis were positive regulation of translation, positive regulation of telomerase RNA localization to Cajal body, translational initiation, histone H2B conserved C-terminal lysine ubiquitination, and glutamate biosynthetic process (Figure 3B). The top five terms in cellular components (CC) analysis were membrane, cytoplasmic stress granule, cytosol, microtubule, and cytoplasm (Figure 3C). The top five terms in molecular function (MF) analysis were RNA binding, mRNA binding, ATPase activity, protein binding, and cadherin binding (Figure 3D). The KEGG pathway analysis revealed that SLC7A11 interacted proteins were enriched in the pathways of spliceosome, ribosome, huntington disease, and diabetic cardiomyopathy (Figure 3E).

Protein-Protein Interaction (PPI) network was constructed based on SLC7A11 binding proteins using STRING website (Figure 3F). We further identified hub genes among SLC7A11 binding proteins using cytoHubba plugin in Cytoscape based on two algorithms (Degree and MCC), and 6 genes including chaperonin containing TCP-1 subunit 4 (CCT4), chaperonin containing TCP-1 subunit 5 (CCT5), eukaryotic initiation factor 4A1 (EIF4A1), glutamyl-prolyl-tRNA synthetase 1 (EPRS), heat shock protein family A member 9 (HSPA9) and ELAV like RNA binding protein 1 (ELAVL1) were selected by both Degree and MCC methods (Figure 3G and 3H). Importantly, co-immunoprecipitation (co-IP) results confirmed the binding between SLC7A11 and ELAVL1 (Figure 3I).

### Identification of the deubiquitinases that regulate SLC7A11 protein expression in ESCC cells

27 deubiquitinase inhibitors are applied to identify the deubiquitinases that regulate SLC7A11 protein expression in ESCC cells (Figure 4A and 4B). Results

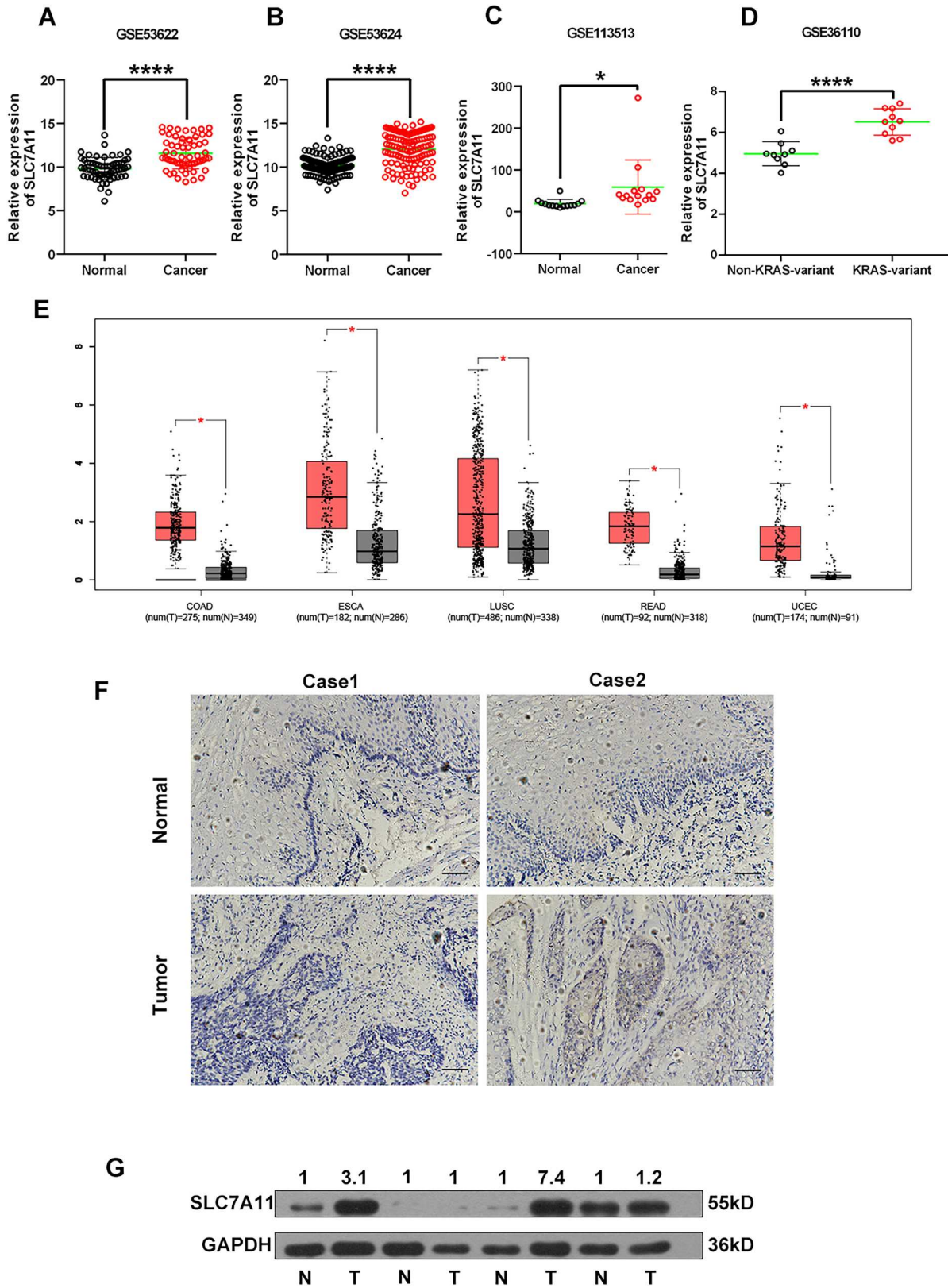


**Figure 1.** SLC7A11 was overexpressed in ESCC tissues. The mRNA levels of SLC7A11 in GSE53622 and GSE53624 ESCC datasets (A and B), GSE113513 CRC dataset (C), and GSE36110 HNSCC dataset (D). (E) The mRNA levels of SLC7A11 in COAD, ESCA, LUSC, READ, and UCEC were analyzed using the GEPIA database. (F) IHC staining of SLC7A11 in ESCC tissues and adjacent normal tissues. (G) The protein levels of SLC7A11 in paired normal and tumor tissues were analyzed using the Western blotting method. \*,  $p < 0.05$ ; \*\*\*\*,  $p < 0.0001$ .



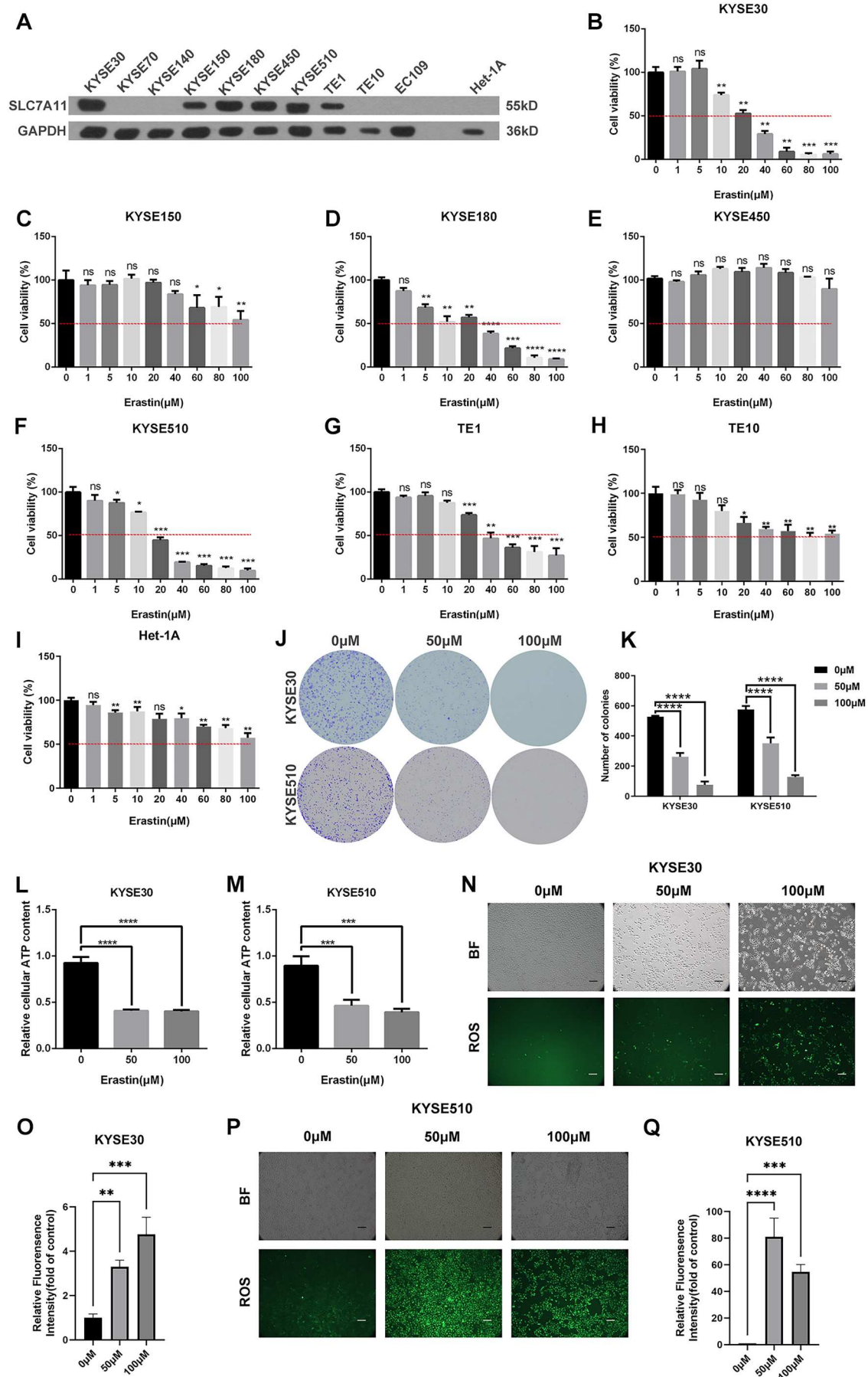


**Figure 2.** Blocking SLC7A11 suppressed the proliferation of ESCC cells. (A) The protein levels of SLC7A11 in ESCC cell lines and the human esophageal normal cell line were detected using the Western blotting method. Cell viabilities (B-I; red line, 50%) and colony formation abilities (J and K) of ESCC cells after Erastin treatment were detected by CCK8 and colony formation methods. Cellular ATP levels (L and M) and ROS levels (N-Q) were evaluated. ns, no significance; \*,  $p < 0.05$ ; \*\*,  $p < 0.01$ ; \*\*\*,  $p < 0.001$ ; \*\*\*\*,  $p < 0.0001$ .



**Table 1.** The interacted proteins of SLC7A11 in ESCC KYSE30 and KYSE510 cell lines.

NO.	Accession	Description (Gene name)	MW	pI	PepCount <sup>1</sup>	Unique PepCount <sup>1</sup>	CoverPercent <sup>1</sup>	PepCount <sup>2</sup>	Unique PepCount <sup>2</sup>	CoverPercent <sup>2</sup>
1	O14979	Heterogeneous nuclear ribonucleoprotein D-like (HNRNPDL)	46436.97	9.59	3	3	0.0476	1	1	0.0238
2	O60716	Catenin delta-1 (CTNND1)	108168.76	5.86	5	5	0.0506	1	1	0.0103
3	O75150	E3 ubiquitin-protein ligase BRE1B (RNF40)	113677.15	5.97	12	12	0.1199	2	2	0.02
4	O75746	Calcium-binding mitochondrial carrier protein Aralar1 (SLC25A12)	74760.96	8.57	2	2	0.0221	1	1	0.0118
5	P00367	Glutamate dehydrogenase 1, mitochondrial (GLUD1)	61397.15	7.66	2	2	0.0376	1	1	0.0197
6	P06576	ATP synthase subunit beta, mitochondrial (ATP5F1B)	56559.22	5.26	2	2	0.0473	5	4	0.1021
7	P07814	Bifunctional glutamate/proline - tRNA ligase (EPRS1)	170588.9	7.02	1	1	0.006	1	1	0.006
8	P08865	40S ribosomal protein SA (RPSA)	32853.68	4.79	1	1	0.0441	1	1	0.0441
9	P0D0X7	Immunoglobulin kappa light chain	23378.81	6.91	1	1	0.0935	16	7	0.4019
10	P16615	Sarcoplasmic/endoplasmic reticulum calcium ATPase 2 (ATP2A2)	114755.63	5.23	1	1	0.106	7	4	0.0441
11	P18085	ADP-ribosylation factor 4 (ARF4)	20510.54	6.6	2	2	0.0889	1	1	0.0333
12	P27816	Microtubule-associated protein 4 (MAP4)	121003.6	5.32	2	2	0.0234	2	2	0.0243
13	P36542	ATP synthase subunit gamma, mitochondrial (ATP5F1C)	32995.66	9.23	4	4	0.1376	2	2	0.0403
14	P38646	Stress-70 protein, mitochondrial (HSPA9)	73679.65	5.87	7	7	0.1105	6	6	0.0913
15	P42166	Lamina-associated polypeptide 2, isoform alpha (TMPO)	75491.15	7.56	5	5	0.098	1	1	0.0231
16	P42677	40S ribosomal protein S27 (RPS27)	9461.04	9.57	1	1	0.1548	1	1	0.0952
17	P42766	60S ribosomal protein L35 (RPL35)	14551.29	11.04	1	1	0.0813	1	1	0.0813
18	P48047	ATP synthase subunit O, mitochondrial (ATP5PO)	23277.05	9.97	1	1	0.0798	2	2	0.1033
19	P48643	T-complex protein 1 subunit epsilon (CTT5)	59670.4	5.45	1	1	0.0148	1	1	0.0092
20	P49411	Elongation factor Tu, mitochondrial (TUFM)	49540.97	7.26	3	3	0.0597	1	1	0.0265
21	P49448	Glutamate dehydrogenase 2, mitochondrial (GLUD2)	61433.27	8.63	2	2	0.0376	1	1	0.0197
22	P50991	T-complex protein 1 subunit delta (CCT4)	57923.6	7.96	1	1	0.0148	1	1	0.0241
23	P51116	Fragile X mental retardation syndrome-related protein 2 (FXR2)	74222.44	5.95	6	6	0.1159	3	3	0.049
24	P51610	Host cell factor 1 (HCF1)	208730.14	7.32	21	19	0.1047	1	1	0.0029
25	P60842	Eukaryotic initiation factor 4A-1 (EIF4A1)	46153.43	5.32	3	3	0.0837	1	1	0.0271
26	P62314	Small nuclear ribonucleoprotein Sm D1 (SNRPD1)	13281.42	11.56	1	1	0.1092	1	1	0.0672
27	P63010	AP-2 complex subunit beta (AP2B1)	104551.36	5.22	1	1	0.0117	1	1	0.0085
28	P67809	Y-box-binding protein 1 (YBX1)	35923.75	9.87	5	3	0.1389	2	2	0.1049
29	P78344	Eukaryotic translation initiation factor 4 gamma 2 (EIF4G2)	102360.69	6.7	1	1	0.011	1	1	0.0088
30	P78527	DNA-dependent protein kinase catalytic subunit (PRKDC)	469083.55	6.75	1	1	0.0022	1	1	0.0027
31	Q00325	Phosphate carrier protein, mitochondrial (SLC25A3)	40094.41	9.45	2	2	0.0552	2	2	0.0525
32	Q01130	Serine/arginine-rich splicing factor 2 (SRSF2)	25476.06	11.86	1	1	0.0362	1	1	0.0362
33	Q01813	ATP-dependent 6-phosphofructokinase, platelet type (PFKP)	85595.14	7.5	1	1	0.0102	1	1	0.0115
34	Q04637	Eukaryotic translation initiation factor 4 gamma 1 (EIF4G1)	175488.95	5.25	1	1	0.0075	1	1	0.0075
35	Q13136	Liprin-alpha-1 (PPF1A1)	135777.22	5.91	20	19	0.1897	15	15	0.1448
36	Q13247	Serine/arginine-rich splicing factor 6 (SRSF6)	39586.34	11.42	1	1	0.0262	1	1	0.0262
37	Q14157	Ubiquitin-associated protein 2-like (UBAP2L)	114533.12	6.61	10	9	0.1058	5	5	0.0589
38	Q14694	Ubiquitin carboxyl-terminal hydrolase 10 (USP10)	87132.74	5.19	3	3	0.0426	1	1	0.0113
39	Q15058	Kinesin-like protein KIF14 (KIF14)	186489.47	8.06	5	5	0.0316	1	1	0.0067
40	Q15717	ELAV-like protein 1 (ELAVL1)	36091.47	9.23	1	1	0.0337	1	1	0.0337
41	Q5RHP9	Glutamate-rich protein 3 (ERIC3)	168464.02	4.84	2	1	0.0039	1	1	0.0039
42	Q5VTR2	E3 ubiquitin-protein ligase BRE1A (RNF20)	113661.11	5.73	21	21	0.2174	8	8	0.0872
43	Q6PKG0	La-related protein 1 (LARP1)	123508.81	8.91	2	2	0.0228	2	2	0.0155
44	Q6ZRR7	Leucine-rich repeat-containing protein 9 (LRRC9)	166909.31	7.66	1	1	0.0034	1	1	0.0041
45	Q71U36	Tubulin alpha-1A chain (TUBA1A)	50135.07	4.94	21	16	0.4545	12	10	0.2705
46	Q71UM5	40S ribosomal protein S27-like (RPS27L)	9477.08	9.57	1	1	0.1548	1	1	0.0952
47	Q7L0Y3	tRNA methyltransferase 10 homolog C (TRMT10C)	47346.38	9.4	1	1	0.0372	1	1	0.0273
48	Q8N365	Circadian-associated transcriptional repressor (CIART)	41442.45	9.49	1	1	0.0182	1	1	0.0182

(Continued)

**Table 1.** Continued.

NO.	Accession	Description (Gene name)	MW	pI	PepCount <sup>1</sup>	Unique PepCount <sup>1</sup>	CoverPercent <sup>1</sup>	PepCount <sup>2</sup>	Unique PepCount <sup>2</sup>	CoverPercent <sup>2</sup>
49	Q8NCA5	Protein FAM98A (FAM98A)	55271.88	9.1	4	3	0.0637	1	1	0.027
50	Q8WWH4	Ankyrin repeat, SAM and basic leucine zipper domain-containing protein 1 (ASZ1)	53457.62	5.6	1	1	0.0105	1	1	0.0126
51	Q92974	Rho guanine nucleotide exchange factor 2 (ARHGEF2)	111541.29	6.89	12	11	0.0882	7	7	0.068
52	Q96E39	RNA binding motif protein, X-linked-like-1 (RBMXL1)	42141.08	9.9	2	2	0.0462	1	1	0.0333
53	Q96H51	Serine/threonine-protein phosphatase PGAM5, mitochondrial (PGAM5)	32004.07	8.88	4	4	0.1107	1	1	0.0242
54	Q9BRL6	Serine/arginine-rich splicing factor 8 (SRSF8)	32287.16	11.72	1	1	0.0284	1	1	0.0284
55	Q9BTA9	WW domain-containing adapter protein with coiled-coil (WAC)	70723.45	9.49	1	1	0.0263	1	1	0.0263
56	Q9BUJ2	Heterogeneous nuclear ribonucleoprotein U-like protein 1 (HNRNPUL1)	95737.39	6.49	3	3	0.0362	1	1	0.0129
57	Q9BY44	Eukaryotic translation initiation factor 2A (EIF2A)	64989.32	9.01	13	13	0.2786	3	3	0.0547
58	Q9HC35	Echinoderm microtubule-associated protein-like 4 (EML4)	108914.94	5.96	17	17	0.1855	3	3	0.0387
59	Q9HCE1	Helicase MOV-10 (MOV10)	113669.91	9	5	5	0.0499	1	1	0.006
60	Q9P258	Protein RCC2 (RCC2)	56083.89	9.02	1	1	0.0287	1	1	0.0192
61	Q9Y230	RuvB-like 2 (RUVBL2)	51155.99	5.49	10	10	0.2138	1	1	0.0194
62	Q9Y265	RuvB-like 1 (RUVBL1)	50227.43	6.02	6	5	0.1294	1	1	0.0241
63	Q9Y520	Protein PRRC2C (PRRC2C)	316907.31	9.17	6	6	0.0228	2	2	0.0079

Note: MW: molecular weight; pI: isoelectric point; PepCount: peptide count; Unique pepcount: unique peptide count; 1: KYSE30; 2: KYSE510.



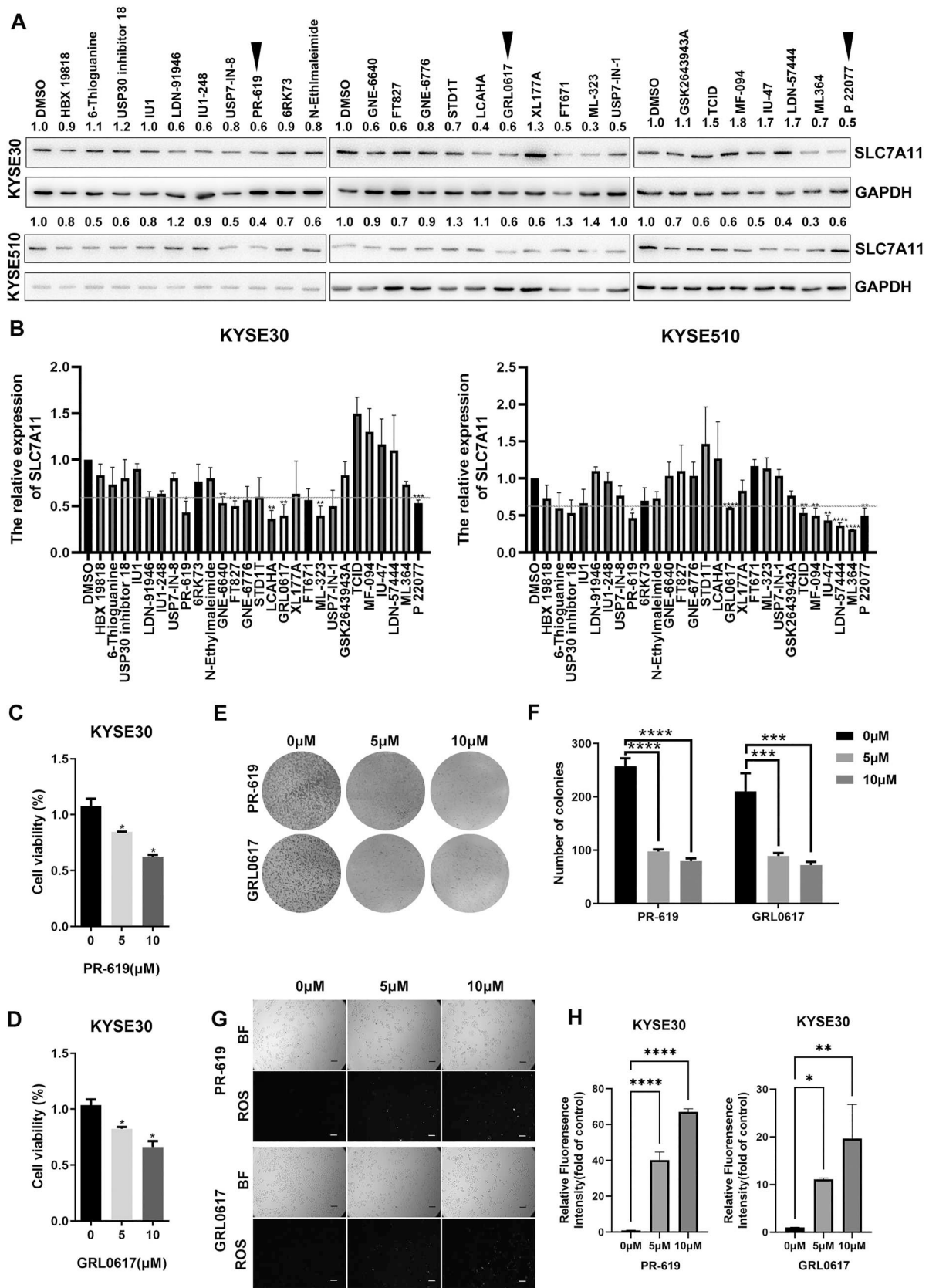


**Figure 4.** Identification of the deubiquitinases that regulate SLC7A11 protein stability in ESCC cells. (A and B) Western blotting assay was used to detect the protein level of SLC7A11 after the deubiquitinase inhibitors treatment. Red line: 0.6. After treating KYSE30 cells with PR-619 and GRL0617 respectively, cell viabilities (C and D), colony formation abilities (E and F), and cellular ROS levels (G and H) were measured. \*,  $p < 0.05$ ; \*\*,  $p < 0.01$ ; \*\*\*,  $p < 0.001$ ; \*\*\*\*,  $p < 0.0001$ .

and cellular ROS level in KYSE30 cells. Results showed that both PR-619 and GRL0617 treatment significantly reduced cell viability and colony formation ability, and improved the cellular ROS level in KYSE30 cells, respectively (Figure 4C-4H).

Next, we analyzed the mRNA expression levels of USP2, USP4, USP5, USP7, and USP8, target genes of PR-619, GRL0617 and P 22077, in ESCC datasets (GSE53622 and GSE53624). In these two datasets, USP5 was significantly overexpressed, but USP2, USP4, and USP7 were remarkably decreased, and USP8 showed opposite changes (Figure 5B-5K).

### **Blocking SLC7A11 decreased ferroptosis-associated molecules GPX4 and DHODH, and also reduced DRP1 and MFN1 in ESCC cells**

Erastin (50 and 100  $\mu$ M) didn't affect the protein expression of SLC7A11 in KYSE30 and KYSE510 cells (Figure 6A-6C). We further investigated whether Erastin regulated other ferroptosis-associated molecules such as GPX4 and dihydroorotate dehydrogenase (DHODH), and both GPX4 and DHODH were downregulated after Erastin treatment (Figure 6D-6H). Importantly, Erastin also decreased the protein expression of dynamin-related protein 1 (DRP1), mitochondrial fusion 1 (MFN1), and pyruvate kinase M2 (PKM2) in KYSE30 and KYSE510 cells (Figure 6I-6O). Western blotting analysis further showed that Erastin treatment reduced protein levels of  $\beta$ -catenin, signal transducer and activator of transcription 3 phosphorylation (p-STAT3) and interleukin 6 (IL-6) in KYSE510 cells (6P-6S).

## **Discussion**

SLC7A11, a key molecule of ferroptosis, is highly expressed in several types of tumors, including ESCC, which has a very low five-year survival rate (Miyata et al. 2009; Feng et al. 2021; Miller et al. 2022), so it is particularly important to understanding the molecular mechanism during esophageal cancer progression. Our results confirmed the high expression of SLC7A11 in ESCC both in mRNA and protein levels. Importantly, we further found that Erastin could significantly reduce the cell viability and colony formation ability of ESCC cells by reducing cellular ATP levels and promoting ROS production. Nevertheless, Erastin treatment didn't affect the protein expression of SLC7A11. Thus, the suppressive effects of Erastin on phenotypes of ESCC cells were probably dependent on the activity of system Xc-. In our study, KYSE30, KYSE510, and KYSE510 cells with a high level of SLC7A11 showed sensitivity to Erastin treatment, however, KYSE450 cells in which

SLC7A11 was also highly expressed showed resistance to Erastin treatment. A previous study reported that the status of intracellular labile iron pool determined the sensitivity of cancer cells to Erastin, and cancer cells with low baseline intracellular labile iron pool showed resistance to Erastin (Battaglia et al. 2022). Therefore, whether low baseline intracellular labile iron pool or other reasons caused KYSE450 cells' resistance to Erastin still needs to be investigated.

Next, we analyzed whether Erastin regulated other ferroptosis-associated molecules. GPX4 and DHODH are crucial regulators in the ferroptosis of cancer cells (Yang et al. 2014; Mao et al. 2021a), and in our study, Erastin treatment decreased the protein levels of GPX4 and DHODH in ESCC cells. Previous studies reported that overexpression of GPX4 indicated poor prognosis of ESCC patients (Shishido et al. 2021), and GPX4 was involved in CysteinyI-tRNA synthetase 1 (CARS1), Ferulic acid (FA), 5-aminolevulinic acid (5-ALA)-induced ferroptosis of ESCC cells (Shishido et al. 2021; Cao et al. 2022; Zhang et al. 2022). A previous study reported that Erastin treatment could promote the protein degradation of GPX4 by chaperone-mediated autophagy (Wu et al. 2019). In GPX4 lowly-expressed cells, inactivation of DHODH potentiated ferroptosis dependently of its catalyzing activity of transforming ubiquinone to ubiquinol (Mao et al. 2021b). DHODH was overexpressed in ESCC tissues and induced nuclear accumulation of  $\beta$ -catenin via binding with the NH2 terminal of  $\beta$ -catenin and abrogating the interaction between  $\beta$ -catenin and glycogen synthetase kinase 3beta (GSK3 $\beta$ ) independently of DHODH catalyzing activity (Qian et al. 2020). Therefore, Erastin led to ferroptosis of ESCC cells via blocking system Xc- and lessening GPX4 and DHODH expression.

IP-MS technology was applied to identify SLC7A11-binding proteins in ESCC and 63 proteins were identified. These SLC7A11-binding proteins were enriched in four signaling pathways, including spliceosome, ribosome, huntington disease, and diabetic cardiomyopathy. Six hub proteins, including CCT4, CCT5, EIF4A1, EPRS, HSPA9, and ELAVL1, were screened out by both Degree and MCC methods among all the SLC7A11-binding proteins. Co-IP assay confirmed the interaction between ELAVL1 and SLC7A11 in KYSE30 and KYSE510 cells. ELAVL1, also known as HuR, could bind the AU-rich element (ARE) in the 3' untranslated region (3'UTR), thus regulate the stability and translation efficiency of mRNA (Wu et al. 2019). ELAVL1 was overexpressed in ESCC, and its downregulation mitigated malignant phenotypes of ESCC cells via inversely regulating IL-18 (Xu et al. 2018). Hypoxia-caused HIF-1 $\alpha$  upregulation suppressed ferroptosis of gastric cancer cells through stabilizing SLC7A11 mRNA by ELAVL1 (Lin

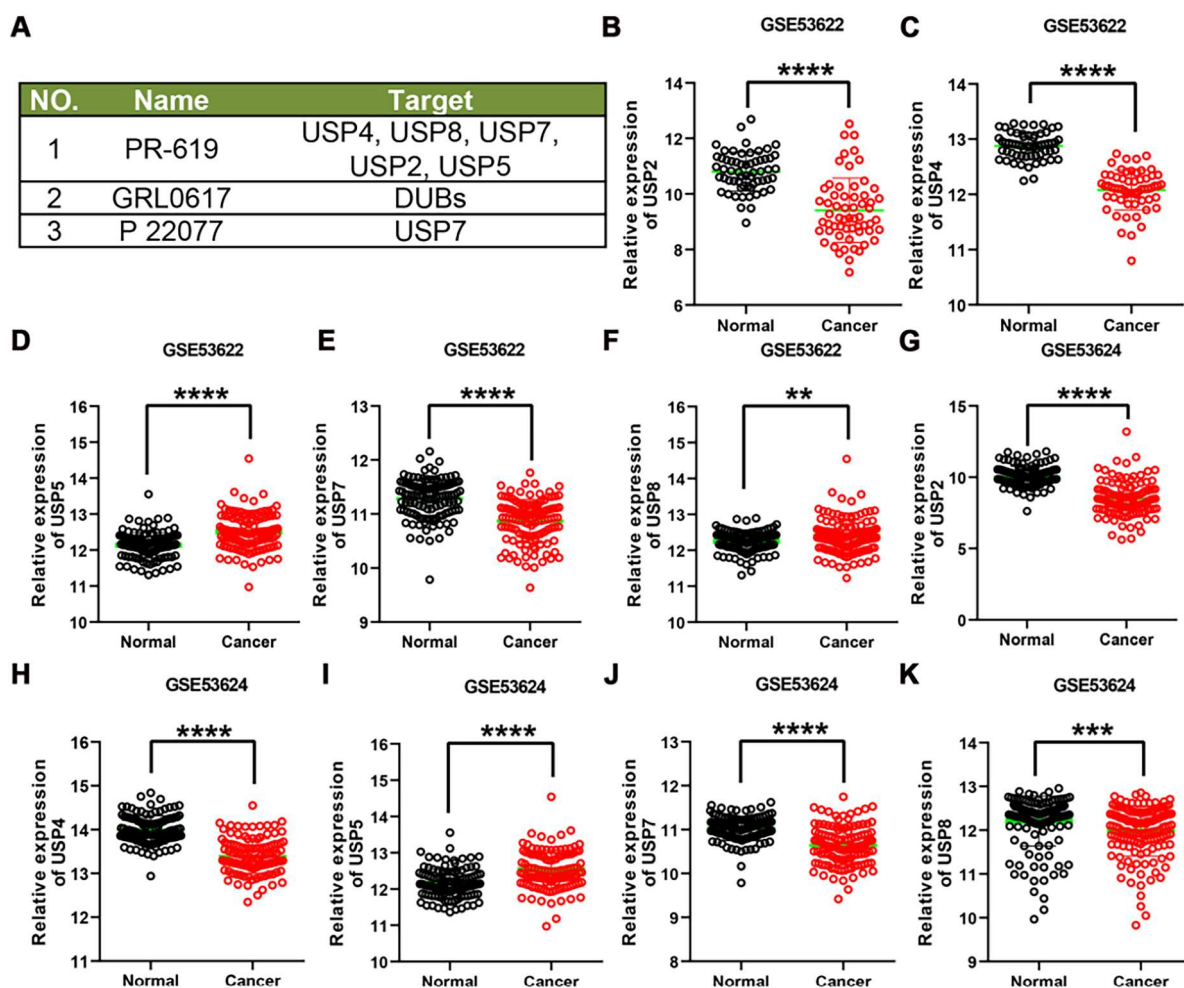


**Figure 5.** USP5 was overexpressed in ESCC tissues. (A) Information about inhibitors and its targets. (B-K) The expression levels of USP2, USP4, USP5, USP7 and USP8 in ESCC tissues were analyzed in GSE53622 and GSE53624 datasets. \*\*,  $p < 0.01$ ; \*\*\*,  $p < 0.001$ ; \*\*\*\*,  $p < 0.0001$ .

et al. 2022). In our study, ELAVL1 was found to bind with SLC7A11 protein, however, the functional roles of interaction between ELAVL1 and SLC7A11 were entirely unclear.

PR-619, GRL0617, and P 22077 were found to lessen at least 40% of the expression level of SLC7A11 in ESCC cells. Among all the targets of these inhibitors, USP5 was significantly overexpressed in ESCC tissues compared with normal tissues possibly indicative of USP5-dependent protein stabilization of SLC7A11 in ESCC cells. As a deubiquitinase, USP5 bound with and stabilized lymphoid-specific helicase (LSH) protein and then increased SLC7A11 expression and weakened ferroptosis of liver cancer cells (Yan et al. 2023). Nevertheless, whether USP5 directly stabilizes SLC7A11 is still needed to be evaluated.

In addition,  $\beta$ -catenin, p-STAT3, and IL-6 were down-regulated after Erastin treatment in KYSE510 cells. IL-6 is one of the critical cytokines in the tumor microenvironment and an activator of the STAT3 pathway. STAT3

plays an important role in tumor cell proliferation and apoptosis (Abroun et al. 2015). In ESCC, activation of the IL-6/STAT3 signaling pathway improved cell proliferation, invasion, and apoptosis resistance and may be developed as the potential therapeutic target in ESCC (Xu et al. 2020; Deng et al. 2021; Chen et al. 2022; Yang et al. 2022).

In conclusion, our study has demonstrated that SLC7A11 was overexpressed in ESCC, and blocking SLC7A11 using Erastin mitigated malignant phenotypes of ESCC cells and downregulated key ferroptosis-associated molecules GPX4 and DHODH, and the stabilization of SLC7A11 was possibly regulated by USP5. However, whether targeting SLC7A11 could be used for ESCC therapy should be investigated in the future.

## Disclosure statement

No potential conflict of interest was reported by the author(s).

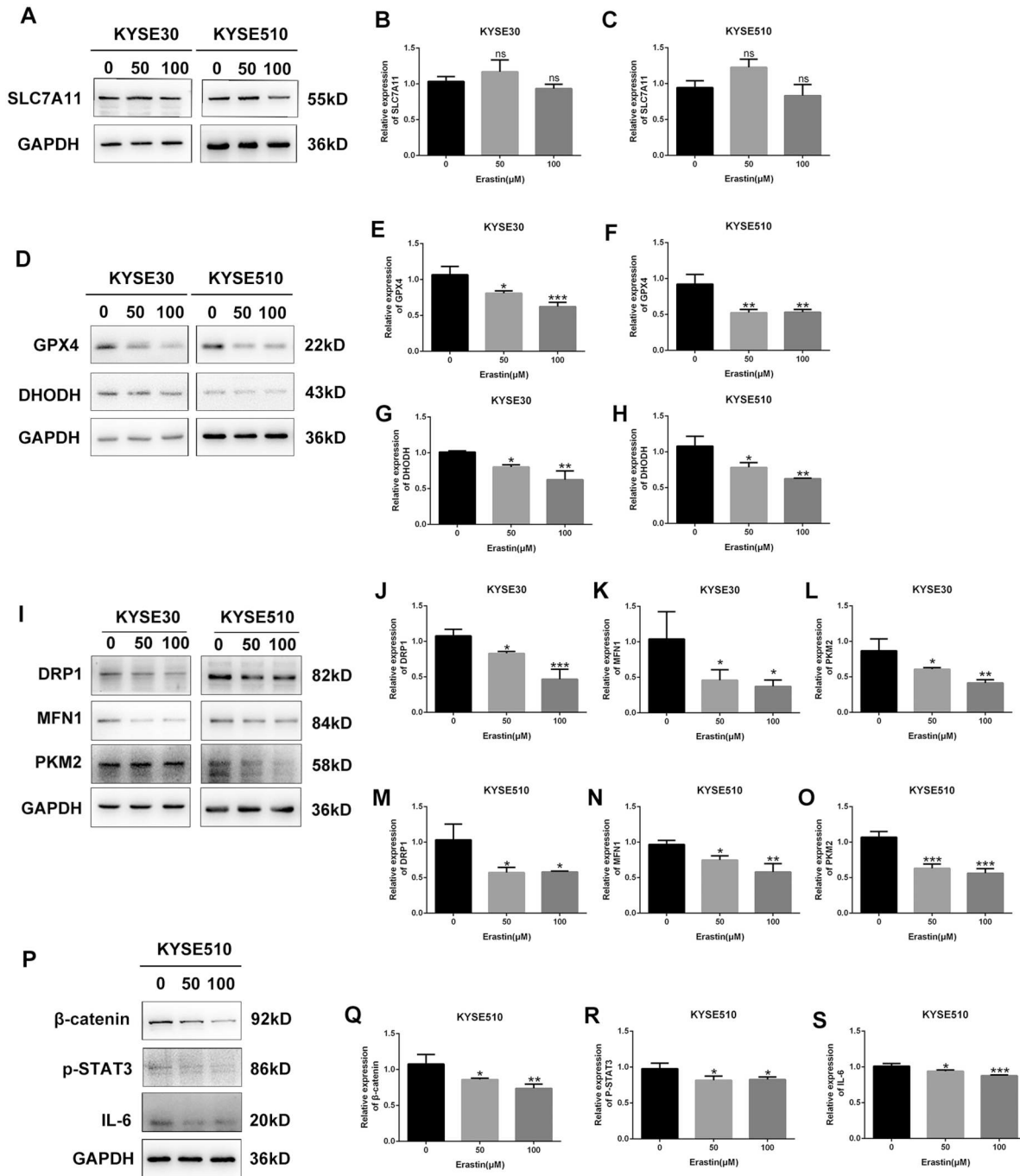


**Figure 6.** Blocking SLC7A11 decreased ferroptosis-associated molecules GPX4 and DHODH, and also reduced DRP1 and MFN1 in ESCC cells. (A-H) The protein levels of ferroptosis-associated genes including SLC7A11, GPX4, and DHODH were detected after Erastin treatment in ESCC cells using Western blotting assay. (I-S) The protein levels of DRP1, MFN1, PKM2,  $\beta$ -catenin, p-STAT3, and IL-6 were detected after Erastin treatment in ESCC cells using Western blotting assay. ns, no significance; \*,  $p < 0.05$ ; \*\*,  $p < 0.01$ ; \*\*\*,  $p < 0.001$ .

## Funding

This study was funded by the [National Natural Science Foundation of China #1] under Grant [No. 82160585]; [Joint Medical Program of Kunming University of Science and Technology #2] under Grant [KUST-KH2022001Z and KUST-PE2022002Z]; [the innovation team of oxidative stress and defense of Yunnan Province #3] under Grant [202305AS350011]; [Yunnan (Kunming) Zhou Demin Expert Workstation Project #4] under

Grant [YSZJGZZ-2020046]; [Chest Disease Clinical Medical Center of The First People's Hospital of Yunnan Province #5] under Grant [No. 2022LCZXKF-XB01].

## References

Abroun S, Saki N, Ahmadvand M, Asghari F, Salari F, Rahim F. 2015. Stats: an old story, yet mesmerizing. *Cell J Fall*. 17:395–411. Epub 2015/10/16.



- Battaglia AM, Sacco A, Perrotta ID, Faniello MC, Scalise M, Torella D, Levi S, Costanzo F, Biamonte F. 2022. Iron administration overcomes resistance to Erastin-mediated ferroptosis in ovarian cancer cells. *Front Oncol*. 12:868351. Epub 2022/04/19.
- Cao Y, Zhang H, Tang J, Wang R. 2022. Ferulic acid mitigates growth and invasion of esophageal squamous cell carcinoma through inducing ferroptotic cell death. *Dis Markers*. 2022:4607966. Epub 2022/10/22.
- Chen T, Xu B, Chen H, Sun Y, Song J, Sun X, Zhang X, Hua W. 2022. Transcription factor NFE2L3 promotes the proliferation of esophageal squamous cell carcinoma cells and causes radiotherapy resistance by regulating IL-6. *Comput Methods Programs Biomed* Nov 226. 107102. Epub 2022/09/16. doi:10.1016/j.cmpb.2022.107102.
- Deng L, Liu J, Chen WD, Wang YD. 2023. Roles of nuclear receptors in esophageal cancer. *Curr Pharm Biotechnol Feb* 2. 24 (12):1489–1503.
- Deng L, Zhang X, Xiang X, Xiong R, Xiao D, Chen Z, Liu K, Feng G. 2021. Nanog promotes cell proliferation, invasion, and stemness via IL-6/STAT3 signaling in esophageal squamous carcinoma. *Technol Cancer Res Treat Jan-Dec*. 20:15330338211038492. Epub 2021/09/15.
- Dixon SJ, Lemberg KM, Lamprecht MR, Skouta R, Zaitsev EM, Gleason CE, Patel DN, Bauer AJ, Cantley AM, Yang WS, et al. 2012. Ferroptosis: an iron-dependent form of nonapoptotic cell death. *Cell* May 25. 149:1060–1072. Epub 2012/05/29. doi:10.1016/j.cell.2012.03.042.
- Feng L, Zhao K, Sun L, Yin X, Zhang J, Liu C, Li B. 2021. SLC7A11 regulated by NRF2 modulates esophageal squamous cell carcinoma radiosensitivity by inhibiting ferroptosis. *J Translational Med* Aug 26. 19:367. Epub 2021/08/28. doi:10.1186/s12967-021-03042-7.
- Han J, Guo X, Zhao L, Zhang H, Ma S, Li Y, Zhao D, Wang J, Xue F. 2023. Development and validation of esophageal squamous cell carcinoma risk prediction models based on an endoscopic screening program. *JAMA Netw Open* Jan 3. 6:e2253148. Epub 2023/01/27.
- Koppula P, Zhang Y, Zhuang L, Gan B. 2018. Amino acid transporter SLC7A11/xCT at the crossroads of regulating redox homeostasis and nutrient dependency of cancer. *Cancer Commun (Lond)* Apr 25. 38:12. Epub 2018/05/17.
- Lin Z, Song J, Gao Y, Huang S, Dou R, Zhong P, Huang G, Han L, Zheng J, Zhang X, et al. 2022. Hypoxia-induced HIF-1 $\alpha$ /lncRNA-PMAN inhibits ferroptosis by promoting the cytoplasmic translocation of ELAVL1 in peritoneal dissemination from gastric cancer. *Redox Biology* Jun. 52:102312. Epub 2022/04/22. doi:10.1016/j.redox.2022.102312.
- Mao C, Liu X, Zhang Y, Lei G, Yan Y, Lee H, Koppula P, Wu S, Zhuang L, Fang B, et al. 2021a. Author correction: DHODH-mediated ferroptosis defence is a targetable vulnerability in cancer. *Nature* Aug. 596:E13. Epub 2021/08/04.
- Mao C, Liu X, Zhang Y, Lei G, Yan Y, Lee H, Koppula P, Wu S, Zhuang L, Fang B, et al. 2021b. DHODH-mediated ferroptosis defence is a targetable vulnerability in cancer. *Nature* May. 593:586–590. Epub 2021/05/14. doi:10.1038/s41586-021-03539-7.
- Miller KD, Nogueira L, Devasia T, Mariotto AB, Yabroff KR, Jemal A, Kramer J, Siegel RL. 2022. Cancer treatment and survivorship statistics, 2022. *CA Cancer J Clin Sep*. 72:409–436. Epub 2022/06/24. doi:10.3322/caac.21731.
- Miyata H, Yoshioka A, Yamasaki M, Nushijima Y, Takiguchi S, Fujiwara Y, Nishida T, Mano M, Mori M, Doki Y. 2009. Tumor budding in tumor invasive front predicts prognosis and survival of patients with esophageal squamous cell carcinomas receiving neoadjuvant chemotherapy. *Cancer* Jul 15. 115:3324–3334. Epub 2009/05/20. doi:10.1002/cncr.24390.
- Pan C, Chen G, Zhao X, Xu X, Liu J. 2022. lncRNA BBOX1-AS1 silencing inhibits esophageal squamous cell cancer progression by promoting ferroptosis via miR-513a-3p/SLC7A11 axis. *Eur J Pharmacol* Nov 5. 934:175317. Epub 2022/10/11. doi:10.1016/j.ejphar.2022.175317.
- Qian Y, Liang X, Kong P, Cheng Y, Cui H, Yan T, Wang J, Zhang L, Liu Y, Guo S, et al. 2020. Elevated DHODH expression promotes cell proliferation via stabilizing  $\beta$ -catenin in esophageal squamous cell carcinoma. *Cell Death Dis* Oct 15. 11:862. Epub 2020/10/17. doi:10.1038/s41419-020-03044-1.
- Sato H, Tamba M, Kuriyama-Matsumura K, Okuno S, Bannai S. 2000. Molecular cloning and expression of human xCT, the light chain of amino acid transport system xc. *Antioxid Redox Signal Winter*. 2:665–671. Epub 2001/02/24. doi:10.1089/ars.2000.2.4-665.
- Shi ZZ, Wang WJ, Chen YX, Fan ZW, Xie XF, Yang LY, Chang C, Cai Y, Hao JJ, Wang MR, et al. 2020. The miR-1224-5p/TNS4/EGFR axis inhibits tumour progression in oesophageal squamous cell carcinoma. *Cell Death Dis* Jul 30. 11:597. Epub 2020/08/01. doi:10.1038/s41419-020-02801-6.
- Shiozaki A, Iitaka D, Ichikawa D, Nakashima S, Fujiwara H, Okamoto K, Kubota T, Komatsu S, Kosuga T, Takeshita H, et al. 2014. xCT, component of cysteine/glutamate transporter, as an independent prognostic factor in human esophageal squamous cell carcinoma. *J Gastroenterol* May. 49:853–863. Epub 2013/06/19. doi:10.1007/s00535-013-0847-5.
- Shishido Y, Amisaki M, Matsumi Y, Yakura H, Nakayama Y, Miyauchi W, Miyatani K, Matsunaga T, Hanaki T, Kihara K, et al. 2021. Antitumor effect of 5-aminolevulinic acid through ferroptosis in esophageal squamous cell carcinoma. *Ann Surgical Oncol* Jul 28. 3996–4006. Epub 2020/11/20. doi:10.1245/s10434-020-09334-4.
- Shu Z, Guo J, Xue Q, Tang Q, Zhang B. 2022. Single-cell profiling reveals that SAA1+ epithelial cells promote distant metastasis of esophageal squamous cell carcinoma. *Front Oncol*. 12:1099271. Epub 2023/01/07.
- Wang L, Wang C, Li X, Tao Z, Zhu W, Su Y, Choi WS. 2023. Melatonin and erastin emerge synergistic anti-tumor effects on oral squamous cell carcinoma by inducing apoptosis, ferroptosis, and inhibiting autophagy through promoting ROS. *Cell Mol Biol Lett* May 2. 28:36. Epub 2023/05/03. doi:10.1186/s11658-023-00449-6.
- Wu M, Tong CWS, Yan W, To KKW, Cho WCS. 2019. The RNA binding protein HuR: A promising drug target for anticancer therapy. *Curr Cancer Drug Targets*. 19:382–399. Epub 2018/11/02.
- Wu Z, Geng Y, Lu X, Shi Y, Wu G, Zhang M, Shan B, Pan H, Yuan J. 2019. Chaperone-mediated autophagy is involved in the execution of ferroptosis. *Proc Natl Acad Sci U S A* Feb 19. 116:2996–3005. Epub 2019/02/06. doi:10.1073/pnas.1819728116.
- Xu X, Song C, Chen Z, Yu C, Wang Y, Tang Y, Luo J. 2018. Downregulation of HuR inhibits the progression of esophageal cancer through Interleukin-18. *Cancer Res Treat Jan*. 50:71–87. Epub 2017/02/25. doi:10.4143/crt.2017.013.

- Xu Z, Tie X, Li N, Yi Z, Shen F, Zhang Y. 2020. Circular RNA hsa\_circ\_0000654 promotes esophageal squamous cell carcinoma progression by regulating the miR-149-5p/IL-6/STAT3 pathway. *IUBMB Life Mar.* 72:426–439. Epub 2019/11/30. doi:10.1002/iub.2202.
- Yan B, Guo J, Wang Z, Ning J, Wang H, Shu L, Hu K, Chen L, Shi Y, Zhang L, et al. 2023. The ubiquitin-specific protease 5 mediated deubiquitination of LSH links metabolic regulation of ferroptosis to hepatocellular carcinoma progression. *MedComm Aug.* 4:e337. Epub 2023/07/26.
- Yang G, Sheng B, Li R, Xu Q, Zhang L, Lu Z. 2022. Dehydrocostus lactone induces apoptosis and cell cycle arrest through regulation of JAK2/STAT3/PLK1 signaling pathway in human esophageal squamous cell carcinoma cells. *Anticancer Agents Med Chem.* 22:1742–1752. Epub 2021/08/07.
- Yang WS, SriRamaratnam R, Welsch ME, Shimada K, Skouta R, Viswanathan VS, Cheah JH, Clemons PA, Shamji AF, Clish CB, et al. 2014. Regulation of ferroptotic cancer cell death by GPX4. *Cell Jan 16.* 156:317–331. Epub 2014/01/21. doi:10.1016/j.cell.2013.12.010.
- Yang YM, Hong P, Xu WW, He QY, Li B. 2020. Advances in targeted therapy for esophageal cancer. *Signal Transduct Target Ther Oct 7.* 5:229. Epub 2020/10/09. doi:10.1038/s41392-020-00323-3.
- Zerbato B, Gobbi M, Ludwig T, Brancato V, Pessina A, Brambilla L, Wegner A, Chiaradonna F. 2023. PGM3 inhibition shows cooperative effects with erastin inducing pancreatic cancer cell death via activation of the unfolded protein response. *Front Oncol.* 13:1125855. Epub 2023/06/01.
- Zhang W, Lin X, Chen S. 2022. Cysteinyl-tRNA synthetase 1 promotes ferroptosis-induced cell death via regulating GPX4 expression. *J Oncol.* 2022(4849174).
- Zhao M, Li M, Zheng Y, Hu Z, Liang J, Bi G, Bian Y, Sui Q, Zhan C, Lin M, et al. 2022. Identification and analysis of a prognostic ferroptosis and iron-metabolism signature for esophageal squamous cell carcinoma. *J Cancer.* 13:1611–1622. Epub 2022/04/05.